


Article

Spectroscopic Characteristics and Coloring Mechanisms of Different Colored Spinel from Myanmar

Lei Zhang, Kui He * and Qingfeng Guo * 

School of Gemology, China University of Geosciences, Beijing 100083, China

* Correspondence: taxihekui@cugb.edu.cn (K.H.); qfguo@cugb.edu.cn (Q.G.)

Abstract: Spinel is a common gemstone that has attracted the attention of gemologists worldwide because of its high refractive index, rich colors and brilliant hues. Myanmar is an important source of spinel. The present paper provides a systematic characterization of the gemological features of different color spinels from Myanmar, with a discussion and analysis of their color causes. The results show that complete octahedral crystal forms can be seen in Myanmar spinel, with the appearance of dissolution, growth motifs and cross-growth of crystals visible on the crystal surfaces. The XRF results show that the Myanmar red and orange spinel samples contain high levels of Cr, with the magenta sample having significant levels of Cr and the orange sample having more V. The blue and purple samples have high levels of Fe. The peaks of the infrared spectrum mainly appear around 841 cm^{-1} , 690 cm^{-1} and 532 cm^{-1} . Raman spectra have peaks mainly around 310 cm^{-1} , 405 cm^{-1} , 663 cm^{-1} and 764 cm^{-1} . According to the UV-Vis spectrum, the color of Myanmar red and orange spinels is mainly due to Cr^{3+} and V^{3+} . When the Cr^{3+} content is higher than the V^{3+} content, the spinels show a red hue; when the V^{3+} content is higher than Cr^{3+} , the spinels have an orange hue. Blue color is due to the charge transfer between Fe^{2+} and Fe^{3+} . The research in this paper has enriched the gemological characteristics of Myanmar spinel and can provide a theoretical basis for its investigation, marketability, design and utilization.

Keywords: Myanmar spinel; gemological characteristics; spectroscopic characteristics; chromogenic element



Citation: Zhang, L.; He, K.; Guo, Q. Spectroscopic Characteristics and Coloring Mechanisms of Different Colored Spinel from Myanmar. *Crystals* **2023**, *13*, 575. <https://doi.org/10.3390/cryst13040575>

Academic Editor: Sergey V. Krivovichev

Received: 7 March 2023

Revised: 22 March 2023

Accepted: 24 March 2023

Published: 28 March 2023



Copyright: © 2023 by the authors. Licensee MDPI, Basel, Switzerland. This article is an open access article distributed under the terms and conditions of the Creative Commons Attribution (CC BY) license (<https://creativecommons.org/licenses/by/4.0/>).

1. Introduction

Spinel is a highly prized gemstone variety that is often featured in major jewelry exhibitions and auctions. In recent years, spinel has gained a great deal of popularity in the market thanks to its colorful and relatively low prices, and it has also attracted the attention of gemologists around the world [1–3]. The composition of the material and its cation distribution have a strong influence on the physical properties of spinel minerals [4]. The crystal structure of spinel belongs to the cubic crystal system, where the divalent oxygen ions contained within the structure are stacked in three dimensions, in a close-packed ionic array with filled one-eighth of tetrahedral and one-half of octahedral interstices [5]. The general formula of spinel can be expressed by AB_2O_4 [1], among which ‘A’ ions are filled in the tetrahedral vacancies, such as Mg^{2+} , Fe^{2+} , Mn^{2+} , Zn^{2+} , Co^{3+} and Ni^{2+} ; B ions are in octahedral vacancies; and trivalent cations are the main ions constituting group ‘B’, such as Al^{3+} , Fe^{3+} and Cr^{3+} [2]. The spinel-type structure can be subdivided into three subtypes according to the distribution of group A and B cations in the structure: orthospinel, represented by the general formula $\text{A}[\text{B}_2]\text{O}_4$; 8 group A divalent cations occupy tetrahedral positions and 16 group B trivalent cations occupy octahedral positions in the unit cell; anti-spinel, represented by the general formula $\text{B}[\text{AB}]\text{O}_4$; 1/2 of the group B trivalent cations occupy the tetrahedral gap, and the remaining 1/2 of the group B trivalent cations and all of the group A divalent cations jointly occupy the octahedral position; mixed type, expressed by the general formula $\text{A}_{1-x}\text{B}_x[\text{A}_x\text{B}_{2-x}]$ [6].

The current gemological research on spinel mainly covers the production origin, gemological characteristics, inclusions, synthetic and heat treatment characteristics identification, spectral characteristics and color genesis of spinel. Most gem-quality spinel deposits can be classified as metamorphic or magmatic by their production. Metamorphic deposits are in most cases formed by contact metamorphism of molten magma intruding into tuffs or dolomites containing inclusions, and are often syngenetic with corundum group minerals. Spinel is often syngenetic with magnesian olivine and diopside. Magmatic deposits spinel occurs mainly in aluminum-rich basic magmatic rocks and is often syngenetic with pyroxene, olivine, magnetite, chromite and platinum group minerals [7]. Most gem spinel are found in impact deposits (secondary deposits). The main sources of spinel are Myanmar, Vietnam, Thailand, Tanzania, Tajikistan, Sri Lanka, Pakistan, Afghanistan, Kenya, Madagascar, Australia, the United States, and Brazil. Among them, and the most famous are red spinel and blue spinel from Myanmar, Thailand and Sri Lanka [8]. Spinel contains numerous inclusions, including solid inclusions (dolomite, magnetite, chromite, flake graphite, columnar apatite, quartz, titanite, zircon, rutile, olivine, pyrrhotite, rutile, epidote) [9]. In addition to inclusions, raw spinel crystals are also commonly found with unhealed cleavage or healed cleavage (fingerprint-like gas-liquid inclusions), growth features (development of growth color bands along octahedral crystal faces), etc. As the value of gem-quality spinel has gone up in the jewelry market, heat treatment techniques for spinel have also come into being. The Gemological Institute of America (GIA) and the Swiss Gemological Research Laboratory (GRS) [10] conducted studies on the heat treatment of spinel in 2004 and 2015, respectively, and the GRS report contained a detailed demonstration of the heat treatment process of spinel. The results showed heat treatment is detectable by Raman spectroscopy and can be semi-quantitatively characterized by the spectral peak parameters (half-height width, spectral peak).

Current research on spinel is focused on chromogenic elements [11–14]. Pure spinel (MgAl_2O_4) is colorless. Due to the abundance of trace elements (transition elements Cr^{3+} , Fe^{2+} , Fe^{3+} , Co^{2+}), spinel displays different colors. The color of the orange and red spinels is mainly attributed to the presence of V^{3+} and Cr^{3+} in the octahedral voids within the structure [15]. Purple spinel is mainly blue (containing Fe and Co) mixed with pink/red (containing Cr); the gray tone of spinel is caused by Fe (Fe^{2+}); green spinel is rare, often blue-green or gray-green, and its main color-causing element is Fe. The blue color of spinel is generally caused by the internal presence of the elements Co or Fe [12]. When the Co and Fe contents are comparable, the effect of Co electron leap on the color is greater than that of Fe. The absorption bands at 545 nm, 550 nm, 580 nm and 625 nm, and the two absorption bands at 556 nm and 588 nm, overlap with those of Fe ion electron leap, resulting in a more intense blue color of spinel [13]. When the Co content is negligible (e.g., <10 ppm), the different shades of gray-blue (from blue-violet to blue-green) are related to the valence and position distribution of Fe ions: when only $^{\text{T}}\text{Fe}^{2+}$ (T means that the ion is in a tetrahedral structure while M means in octahedral) is present, the spinel is violet-blue due to the electron leap; when the concentration of $^{\text{M}}\text{Fe}^{3+}$ increases, the absorption at 588 nm makes the spinel pure blue, and when the concentration of $^{\text{M}}\text{Fe}^{2+}$ and $^{\text{M}}\text{Fe}^{3+}$ increases, the spinel is greenish-blue due to the charge transfer of $\text{Fe}^{2+}\text{-Fe}^{3+}$ at 667 nm. Completely colorless spinel is rare, often with pinkish tones due to Cr content or grayish tones due to Fe^{2+} content [16]. The type of spinel optical absorption spectrum is largely determined by these specific elements. For example, the blue, pink and green iron-rich spinel crystals, which despite the wide variation in their colors produce relatively similar spectra from optical absorption, all have strong UV-edge absorption and a range of weaker absorption bands. Besides this, the variance in color from pink to blue and green spinel samples depends on the increase in Fe^{2+} (primary) and Fe^{3+} content (secondary), which is responsible for the enhanced absorption in the UV-edge.

Myanmar is the most famous source for medium/small-sized red spinels [1], so studies on Myanmar spinels have focused on the red variety 'Jedi' [3,8]. Higher levels of Zn compared to other origins give the Myanmar 'Jedi' spinel a more fluorescent appearance,

giving it a neon and hot pink tint [3]. The geological deposits of spinel in Myanmar have a long history and are mainly found in the three production areas of Mogok, Ywathit and Namya. The 'Mogok Stone Tract' in Mandalay District is the main spinel-producing area in Myanmar and includes several areas around Mogok. Spinel is found in abundance in corundum deposits [17]. The Mogok metamorphic belt is known geotectonically for its high temperature plastic deformation, which was formed around the Oligocene and post-Miocene and is associated with the oblique collision of the India-Eurasia plate [18]. Spinel often occurs with rubies in mines, and many co-occurring minerals can be found in the deposit, including various mica minerals, marble, graphite, pyrite, sphene and so on [19,20]. Studies on the geology of spinel deposits in Myanmar are well-established and much research has been carried out on the red spinels of Myanmar; however, there remains a relative lack of comparative studies on the different colors of spinel from Myanmar.

In the present study, seven raw spinels of different colors from Myanmar were selected, and their surface morphology and crystal shape were observed under the microscope. An X-ray fluorescence spectrometer (EDXRF), Fourier transform infrared spectrometer (FTIR), UV-Vis spectrophotometer and Raman spectroscopy were employed to obtain a systematic examination of the color causes in natural spinel samples from Myanmar. This paper enriches the theoretical study of the different colors of Myanmar spinel by examining the chromogenic elements and characteristic spectra of Myanmar spinel. In addition, this study provides a theoretical basis for the identification and classification of Myanmar spinels by observing and collating their crystallographic characteristics.

2. Materials and Methods

2.1. Materials

Figure 1 shows seven samples of natural spinel from Myanmar in pink (M1), violet (M2), orange (M3,) orange-violet (M4), red (M5) and blue (M6, M7). Samples M1 and M2 have a very complete octahedral crystal shape. M3 and M5 have a fragmentary appearance with some internal fissures. M4, M6 and M7, which have undergone longer river transport, are better-rounded and have a pebbly appearance.

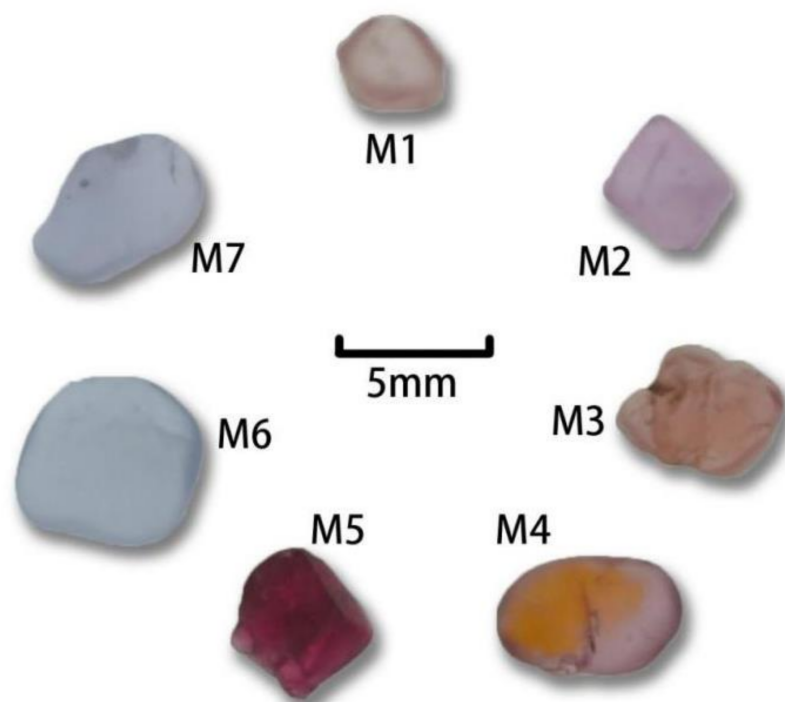


Figure 1. Spinel samples from Myanmar.

2.2. Methods

Conventional gemological features were measured at China University of Geosciences Beijing (CUGB) Gemological Experimental Teaching Centre. Measure the specific gravity with the hydrostatic weighing method. The samples were observed under LW and SW using UV fluorescent lamps, and the luminescence of the samples under LW was photographed using Diamond View. Microscopic observation was carried out using a GI-MP22 gemological photographic microscope.

The data of energy dispersive X-ray fluorescence (XRF) were measured at China University of Geosciences Beijing (CUGB) Gemological Experimental Teaching Centre. The instrument used was EDX-7000 energy dispersive X-ray Fluorescence Spectrometer produced by Shimadzu manufacturer in Japan. The experimental test conditions were: element analysis range was (13)Al-(92)U, accuracy 0.1 ppm, and the test environment was vacuumized before the test.

A UV-Vis spectrophotometer of the model UV-3000 produced by the Shimadzu company in Japan was used, situated in the Gemological Experimental Teaching Centre of the China University of Geosciences Beijing (CUGB). The experimental test method was the transmission method, the test range was 200–900 nm, the light source conversion wavelength was 310 nm, the grating conversion wavelength was 720 nm, and the sampling interval was 0.1 s.

Fourier transform infrared spectroscopy was performed at the China University of Geosciences Beijing (CUGB) Gemological Experimental Teaching Centre. The instrument used for the experiment was the BRUKER Fourier transform infrared spectrometer-Bruker Tensor 27, manufactured by BRUKER Spectrometer, Germany. The experimental conditions were as follows: Using the reflection method for testing, temperature range: 18–35 °C, humidity range: less than 70%, resolution: 4 cm⁻¹, grating set to 6 mm, 10 KHz, spectral range: 400–2000 cm⁻¹, number of scans per sample: 32.

Raman spectroscopy was performed at the China University of Geosciences Beijing (CUGB) Gemological Experimental Teaching Centre, using a HORIBA LabRAM HR-Evolution Raman spectrometer. Microscope with ×50 objectives was used to focus on the samples. The sample was not polished due to its small size, but a smoother surface was sought for the actual inspection. The laser beam was perpendicular to the surface of the sample. The Raman spectrometer recorded in the 200–1000 cm⁻¹ range and with 4 cm⁻¹ resolution, with an excitation light source $\lambda = 532$ nm and 3 s exposure time.

3. Results and Discussion

3.1. Gemological and Crystallographic Characteristics

The conventional gemological characteristics of Myanmar spinels are shown in Table 1. Seven spinel samples were tested, and the specific gravity of the samples ranged from 3.45 to 3.58. The luminescence of the samples under long-wave UV radiation was observed under the Diamond View. As shown in Figure 2, an intense red fluorescence was observed for the pink, red and orange samples. The red sample M5 had the most intense red fluorescence, indicating a high Cr content. The violet sample showed low fluorescence, especially the violet part of the bi-color sample M4, which was barely visible. The blue samples showed an absence of fluorescence under the Diamond View.

As shown in Table 1, seven samples of Myanmar spinel were observed under the Chelsea color filter and subtle hue variations were observed in some samples. For example, the violet sample M2 shows a pinkish tint under the Chelsea color filter. It should be noted that the red sample M5 shows a bright-red hue under the Chelsea color filter. This feature can be used to quickly distinguish spinel from ruby samples, as ruby with a similar color does not usually show such an intense red hue under the Chelsea color filter. The remaining samples M1, M3, M4, M6 and M7 show no significant hue change under the Chelsea color filter. Using a grating spectroscope (hand-held), the sample was observed to have a distinct Cr absorption spectrum in the red sample M5, as evidenced by two distinct absorption lines in the red region at approximately 686 nm and 675 nm, and a broader absorption band

in the green and violet regions. Using a hand-held spectroscope to observe samples M6 and M7, a Fe absorption pattern can be observed, demonstrated by some distinct absorption lines in the purple spectral region. No significant absorption lines are observed using a hand-held spectroscope in the other samples due to their too-light color and too-small size.

Table 1. Gemological characteristics of the samples.

Sample	Color	Weight (c t)	Specific Gravity	Fluorescence (LW)	Chelsea Color Filter	Grating Spectroscope (Hand-Held)
M1	Pink	0.228	3.45	Dark red	No change	/
M2	Light violet	0.338	3.56	Dark red	Pink tones	/
M3	Orange	0.586	3.55	Red	No change	/
M4	Orange-Violet	0.727	3.55	Bright Red	No change	/
M5	Red	0.377	3.59	Bright Red	Bright red tones	Chromium absorption
M6	Light blue	0.515	3.58	None	No change	/
M7	Blue	0.394	3.58	None	No change	Ferrum absorption

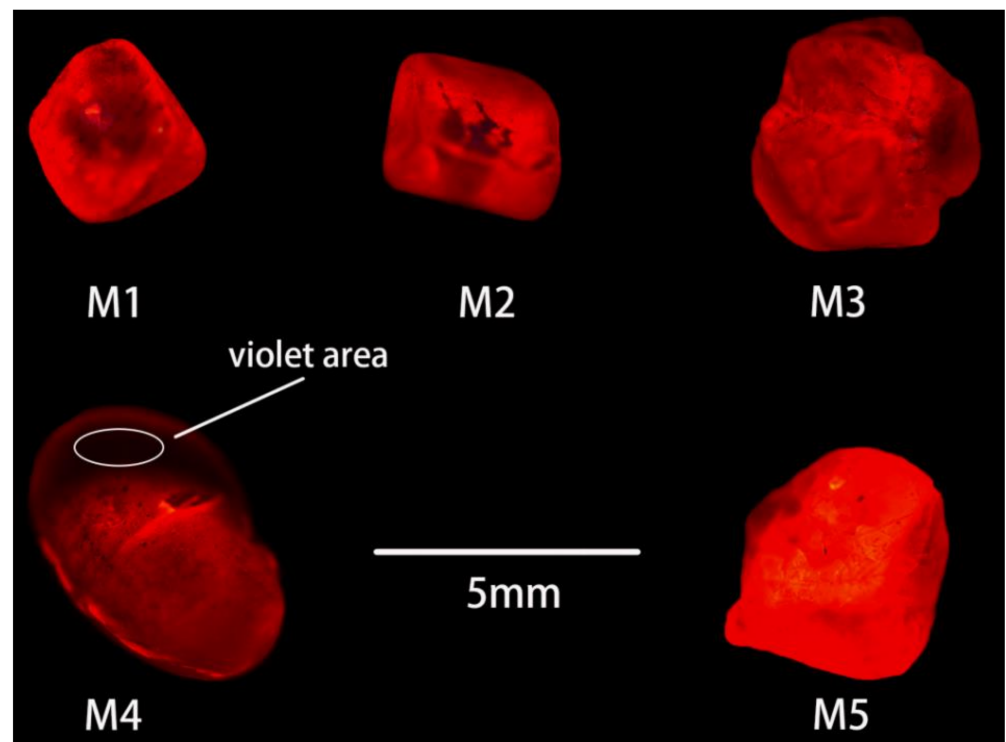


Figure 2. Fluorescence of samples under the Diamond View. (M means “Myanmar”).

As shown in Figure 3a, the typical octahedral crystal shape of spinel can be seen when sample M1 is viewed under the microscope. Figure 3b demonstrated a distinctly soluble appearance and the peculiar triangular growth motifs of spinel crystals that are on the surface of M1. In Figure 3c, it can be clearly observed that inverted triangular-shaped growth pits are distributed on the crystal surface of sample M2. In Figure 3d, M5 can be observed with a tetrahedral angular inward concavity that results from the intercalated growth of the spinel crystal.

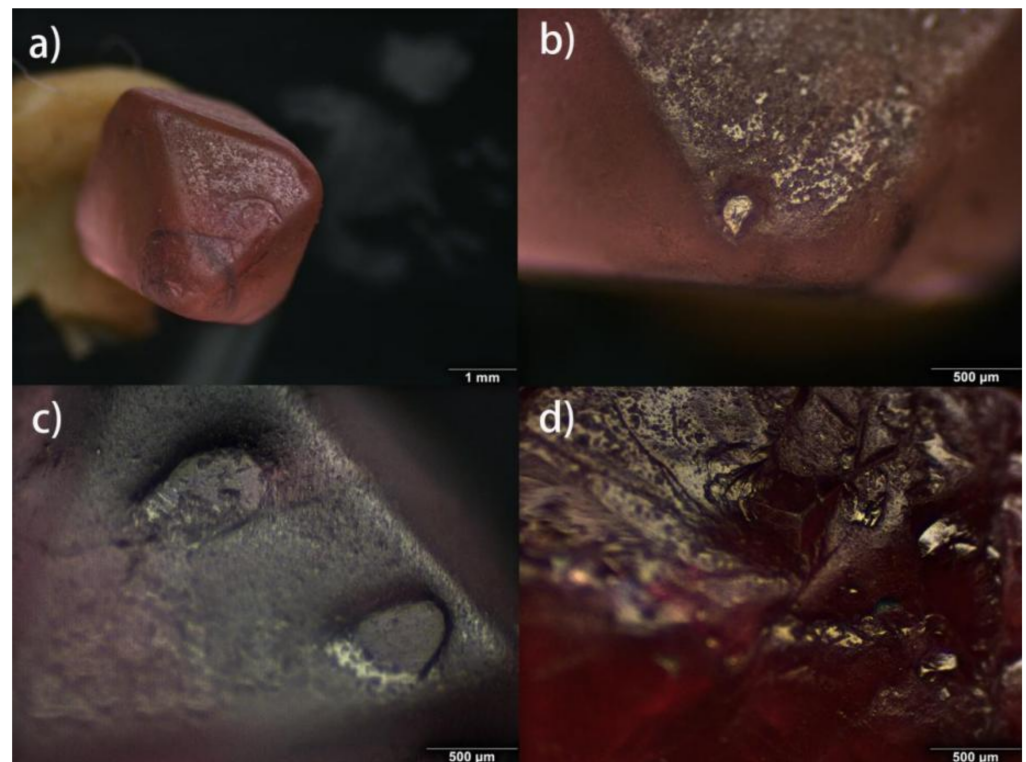


Figure 3. (a) Octahedral crystal (M1) (b); abraded appearance (M1); (c) inverted triangular growth pits (M2); (d) cross-growth phenomenon of crystals (M5).

3.2. Composition Analysis of Myanmar Spinel X-ray Fluorescence Spectroscopy (XRF)

According to Table 2, the main elements of Myanmar spinel are Mg and Al, and the trace elements are mainly Cr, Fe, V, Ti, Mn, Ni and Zn, with Mn and Ti at a lower level. The Al_2O_3 content is around 65%, while the MgO content is around 30%. The main determinant of the color of Myanmar spinel is the content of elemental Cr, followed by the concentration of Fe and V. Cr was the element that mainly caused the red color, with the red sample M5 having much higher levels of Cr than the other samples. The orange sample M3 has a slightly higher V content, while the blue samples M6 and M7 have significantly higher levels of Fe to the other samples. In short, the test results show that the trace element content of the samples varies by colors, the red-orange spinel containing more Cr and V while the blue-violet has a higher Fe content [21].

Table 2. X-ray fluorescence spectral analysis data of different colored Myanmar spinels (wt %).

Sample Number	Color	Al_2O_3	MgO	Cr_2O_3	V_2O_5	Fe_2O_3	ZnO	SiO_2	SO_3	TiO_2
M1	pink	68.311	28.501	0.161	0.173	0.118	0.087	1.667	0.917	ND
M2	violet	57.808	25.346	0.297	0.181	0.739	1.980	2.504	0.956	ND
M3	orange	66.665	30.3271	0.076	0.489	0.077	0.084	1.260	0.939	ND
M4	orange-violet	67.507	29.809	0.148	0.038	0.399	0.079	1.079	0.822	ND
M5	red	65.668	30.229	1.537	0.277	0.124	0.051	1.852	ND	0.149
M6	blue	69.355	18.028	0.230	0.046	1.559	0.610	5.162	4.666	0.081
M7	blue	69.576	16.238	ND	0.312	1.901	0.159	5.284	6.340	0.044

3.3. Spectroscopy Analysis of Myanmar Spinel

3.3.1. Fourier Transform Infrared Spectroscopy (FTIR)

It is the highly symmetrical group of cubic centroids that gives spinel its structure, which is due to the fact that spinel belongs to the fully symmetrical isometric crystal system. This is why only four vibrational modes appear in the infrared spectrum of spinel in the range from 400 to 1000 cm^{-1} [22]. In the structure of spinel, one tetrahedron shares oxygen atoms with three octahedra, so that neither the oxygen tetrahedron nor the octahedron vibrations can occur independently. The two higher-frequency vibrations in the spinel infrared spectrum do not correlate well with the mass of the spinel cations, while the two lower-frequency vibrations correlate closely with the relative displacement between the cations. All four vibrational modes are affected by $\text{Al}^{3+}\text{-O}$ bonding forces, with the F^3_{1u} and F^2_{1u} frequencies being affected by the Al mass—due to the larger Al^{3+} mass, it will be more involved in the F^2_{1u} vibration. In addition, F^4_{1u} will be more sensitive to the mass of Mg [23].

Seven samples were pretreated by surface smoothing and then tested by FTIR spectroscopy; the results are illustrated in Figure 4. As shown in Figure 4, the infrared spectra of the different colors of Myanmar spinel have similar peaks at 478 cm^{-1} , 532 cm^{-1} , 586 cm^{-1} , 690 cm^{-1} and 841 cm^{-1} , respectively. Near 841 cm^{-1} is a high frequency band caused by oxygen ion vibrations [24]. Peaks at 532 cm^{-1} and 586 cm^{-1} are vibrations from Al-O bond stretching. It is notable that the FTIR spectra of the seven different colored samples show a high degree of consistency, with similar peak and trough positions, from which it can be deduced that color has no effect on their FTIR spectra.

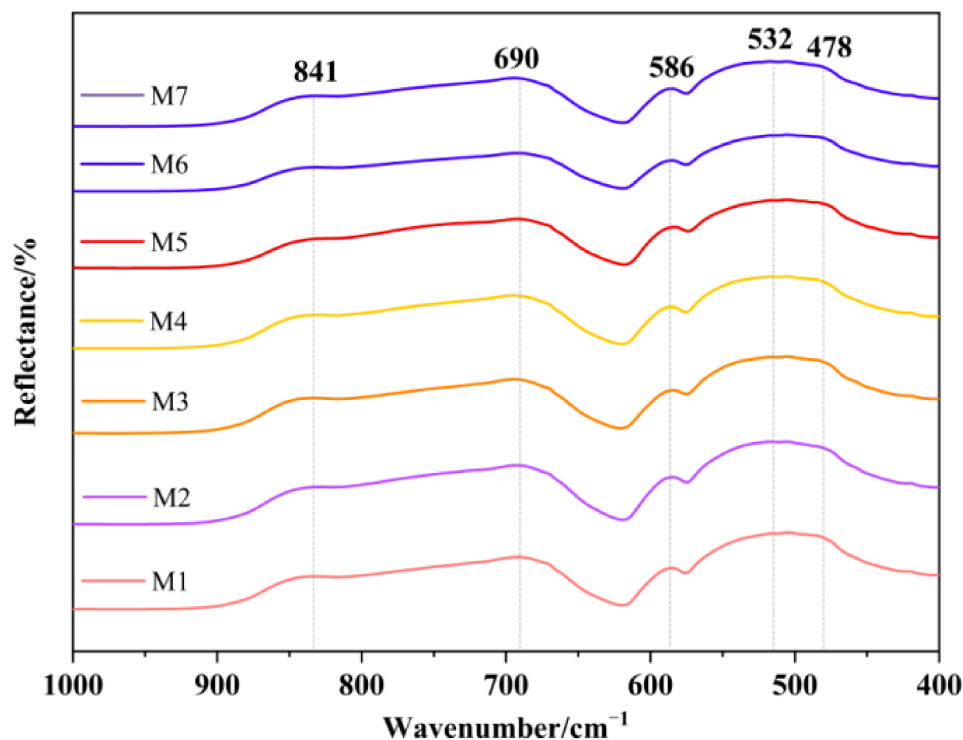


Figure 4. FTIR spectra of different colored spinels from Myanmar.

3.3.2. Raman Spectra

Figure 5 demonstrates the Raman spectroscopy profiles of the seven samples. As shown in Figure 5, the Raman spectra of the seven spinel samples showed a consistent pattern, composed mainly of four intense and well-defined bands, which were situated at 310 cm^{-1} , 405 cm^{-1} , 663 cm^{-1} and 764 cm^{-1} . The peak Eg at 405 cm^{-1} shows that all

seven samples are Mg-Al spinel [25]. In addition, the residual peaks at 310 cm^{-1} , 663 cm^{-1} and 764 cm^{-1} correspond to the signature peaks of $T_{2g}(1)$, $T_{2g}(2)$, A_{1g} , respectively [26–28].

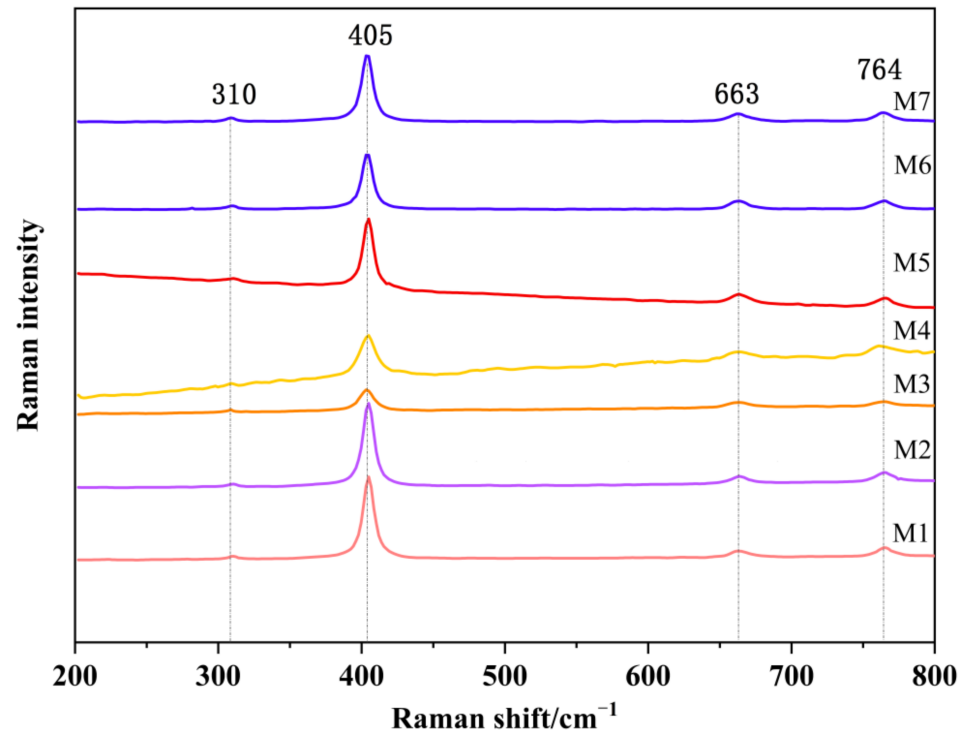


Figure 5. Raman spectra of different colored spinels from Myanmar.

3.3.3. UV-Vis Spectroscopy

The UV-Vis spectrophotometer was used to test the pink-red spinel samples (M1 M3 M4 M5), and Figure 6 shows the absorption of the samples.

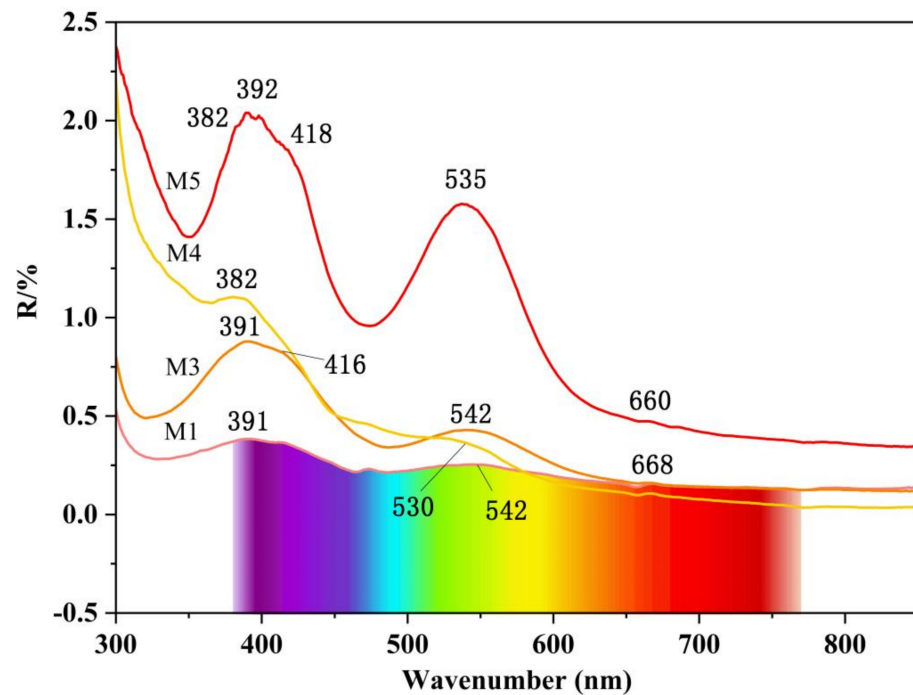


Figure 6. UV-Vis spectra of pink-red spinels. (M means “Myanmar”).

Pink sample M1 shows a similar position of the absorption peak to the red sample M5, but the intensity is weaker. Table 3 shows the Electronic transition for different positions of UV-Vis absorption. Comparing Table 3, it can be seen that the absorption peaks of the red sample M5 belonging to Cr^{3+} are obvious, with three peaks attributed to spin-allowed leap at ${}^4\text{A}_{2g} \rightarrow {}^2\text{T}_{1g}(\text{F})$ 382 nm (b), spin-allowed leap ${}^4\text{A}_{2g} \rightarrow {}^2\text{T}_{1g}(\text{F})$ at 418 nm (d) and spin-allowed leap ${}^4\text{A}_{2g} \rightarrow {}^2\text{T}_{2g}(\text{F})$ at 535 nm (e). The UV-Vis absorption spectra of the orange samples M3 and M4 have a weak absorption band in the blue-violet and green regions, meaning that more red-to-yellow-orange light passes through relative to the UV-blue region, giving the sample an orange-yellow color. Figure 7 a,b shows the Band analysis, which used the Gaussian splitting function, of the UV-Vis spectra of M3 (a) and M5 (b). As in shown in Figure 7, the c and f absorption bands are more pronounced in the orange sample, suggesting that the orange color shown by the Myanmar spinel is mainly due to the higher V^{3+} content in the composition, which may have been greater than that of the Cr^{3+} . In short, the presence of Cr^{3+} and V^{3+} ions gives spinel a red or orange color. At higher levels of Cr^{3+} , the spinel appears pink-red; however, when the concentration of V^{3+} is high, the absorption in the yellow-green light region diminishes and the spinel develops an orange hue.

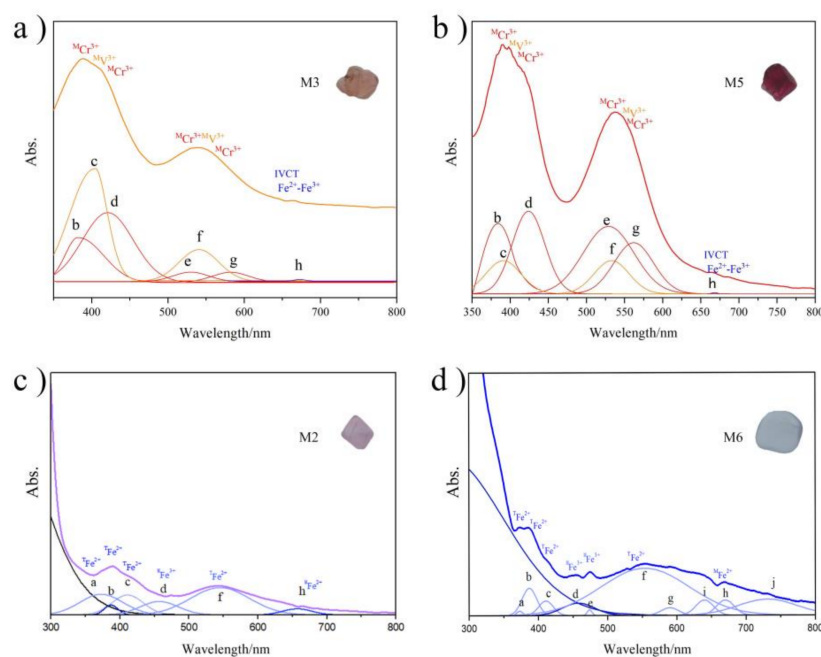


Figure 7. Band analysis of UV-Vis spectra of M3 (a), M5 (b), M2 (c) and M6 (d).

Table 3. UV-Vis spectral peak positions of the red series samples M1 M3 M4 M5 [29–32].

Sample	M1 Pink	M3 Orange	M4 Orange	M5 Red	Assignment	Electronic Transition
a	/	/	/	/	MCr^{3+}	Spin-forbidden ${}^4\text{A}_{2g}({}^4\text{F}) \rightarrow {}^2\text{T}_{1g}({}^2\text{G})$
b	/	/	382	382	MCr^{3+}	Spin-allowed ${}^4\text{A}_{2g} \rightarrow {}^2\text{T}_{1g}(\text{F})$
c	391	391	390	392	MV^{3+}	Spin-allowed ${}^3\text{T}_{1g}(\text{F}) \rightarrow {}^3\text{T}_{1g}(\text{P})$
d	410	416	/	418	MCr^{3+}	Spin-allowed ${}^4\text{A}_{2g} \rightarrow {}^2\text{T}_{1g}(\text{F})$
e	/	/	530	535	MCr^{3+}	Spin-allowed ${}^4\text{A}_{2g} \rightarrow {}^2\text{T}_{2g}(\text{F})$
f	542	542	/	/	MV^{3+}	Spin-allowed ${}^3\text{T}_1(\text{F}) \rightarrow {}^3\text{T}_2(\text{F})$
g	/	/	/	/	MCr^{3+}	Spin-allowed ${}^4\text{A}_{2g} \rightarrow {}^2\text{T}_{2g}(\text{F})$
h	669	668	668	660	$\text{Fe}^{2+}\text{-Fe}^{3+}$	$\text{Fe}^{2+}\text{-Fe}^{3+}$ charge transfer
i	/	/	/	/	MFe^{2+}	Spin-allowed ${}^5\text{T}_{2g} \rightarrow {}^5\text{E}_g$

The UV-Vis spectra of purple sample M2, blue sample M6 and the results of the peak splitting process are shown in Figure 7c,d, and the corresponding attribution of each peak position is shown in Table 4. According to Figure 7c,d, the blue and purple spinels have a different UV-Vis spectral pattern to the red series of spinels. In the 330 nm–400 nm region, corresponding to the blue and purple regions of visible light, a more intense absorption is seen, which is due to the charge transfer leap from O^{2-} to Fe^{2+} and O^{2-} to Fe^{3+} . According to Figure 7c, the absorption band f at 555 nm is dominant in purple sample M2. According to Figure 7d, the blue sample M6 has a more pronounced absorption band f at 554 nm, which is attributed to Fe^{2+} in the T site, causing strong absorption in the green-yellow region and more visible light passing through in the blue region, making the sample a blue color.

Table 4. UV-Vis spectral peak positions of the blue series samples M2, M6 [29–32].

Sample	M2 Violet	M6 Blue	Assignment	Electronic Transition
a	373	373	TFe^{2+}	Spin-forbidden ${}^5E \rightarrow {}^3E$
b	387	387	TFe^{2+}	Spin-forbidden ${}^5E \rightarrow {}^3T_1, {}^3T_2$
c	411	411	TFe^{2+}	Spin-forbidden ${}^5E \rightarrow {}^3T_1$
d	457	458	MFe^{3+}	${}^6A_{1g} \rightarrow {}^4A_{1g}, {}^4E_g$
e	/	474	MFe^{3+}	
f	555	554	TFe^{2+}	Spin-forbidden ${}^5E \rightarrow {}^3T_2$
g	/	590	TFe^{2+}	Spin-forbidden ${}^5E \rightarrow {}^3T_2$
h	657	670	MFe^{2+}	$Fe^{2+}-Fe^{3+}$ charge transfer

4. Conclusions

In summary, the gemological, crystallographic, compositional and spectral characteristics of the Myanmar spinel samples were systematically analyzed using basic gemological instruments and modern testing techniques. Complete octahedral crystal morphology is visible in some samples, with the appearance of dissolution, growth motifs and cross-growth of crystals visible on the crystal surfaces. The average specific gravity of spinel from Myanmar is 3.551, and under long-wave ultraviolet light the red series shows significant fluorescence, while the blue-violet series shows no significant fluorescence. In contrast to existing scholarly studies of spinel (Andreozzi et al. 2019 [15]), this paper focuses on the spectroscopic and gemological characteristics of different colors of spinel from Myanmar—including red, orange, purple and blue, systematically discussed the spectra and chromogenic elements of them. The infrared spectra (FTIR) of the different colors of Myanmar spinel samples have similar peaks at 478 cm^{-1} , 532 cm^{-1} , 586 cm^{-1} , 690 cm^{-1} and 841 cm^{-1} , respectively. Raman spectra of the seven spinel samples also showed a consistent pattern, which was situated at 310 cm^{-1} , 405 cm^{-1} , 663 cm^{-1} and 764 cm^{-1} . The UV-Vis spectra of the different colored samples varied considerably, indicating a strong correlation between the color of the sample and the particular element. According to the UV-Vis spectrum, the color of Myanmar red and orange spinels was mainly due to Cr^{3+} and V^{3+} . When the Cr^{3+} content was higher than the V^{3+} content, the spinels showed a red hue; when the V^{3+} content was higher than Cr^{3+} , the spinels had an orange hue. The causes of blue and purple are mainly attributed to the charge transfer between Fe^{2+} and Fe^{3+} . This is very different from the Vietnam blue spinel, whose blue color is caused by Co^{2+} . The conclusions of this paper facilitate the regulation of the different colors of spinel in Myanmar and can be used as a theoretical foundation for the grading or origin tracing of Myanmar spinel.

Author Contributions: L.Z., writing-original draft preparation and formal analysis; K.H., review and editing; Q.G., review and editing; All authors have read and agreed to the published version of the manuscript.

Funding: This research received no external funding.

Institutional Review Board Statement: Not applicable.

Informed Consent Statement: Not applicable.

Data Availability Statement: Not applicable.

Conflicts of Interest: The authors declare no conflict of interest.

References

1. Zhang, Y.; Zhu, J.R.; Yu, X.Y. A Comparative Study of the Gemological Characteristics and Inclusions in Spinel from Myanmar and Tajikistan. *Crystals* **2022**, *12*, 617. [[CrossRef](#)]
2. Pluthametwisute, T.; Wanthanachaisaeng, B.; Saiyasombat, C.; Sutthirat, C. Minor Elements and Color Causing Role in Spinel: Multi-Analytical Approaches. *Minerals* **2022**, *12*, 928. [[CrossRef](#)]
3. Zhao, L.P.; Li, G.; Weng, L.Q. Gemological and Spectroscopic Characteristics of “Jedi” Spinel from Man Sin, Myanmar. *Minerals* **2022**, *12*, 1359. [[CrossRef](#)]
4. Bosi, F.; Biagioni, C.; Pasero, M. Nomenclature and classification of the spinel supergroup. *Eur. J. Mineral.* **2019**, *31*, 183–192. [[CrossRef](#)]
5. Hill, R.J.; Craig, J.R.; Gibbs, G.V. Systematics of the spinel structure type. *Phys. Chem. Miner.* **1979**, *4*, 317–339. [[CrossRef](#)]
6. Li, S.R. *Crystallography and Mineralogy*; Geological Publishing House: Beijing, China, 2008.
7. Wang, C.Q.; Zhang, L.K. *Gemmology*; Geological Publishing House: Beijing, China, 2017; p. 380.
8. Vincent, P. Hunting for “Jedi” Spinel in Mogok. *Gems Gemol.* **2014**, *50*, 46–57.
9. Günelin, E.J.; Koivula, J.I. *Photoatlas of Inclusion in Gemstones*; Da Zhi Publishing House: Taiwan, China, 1995; Volume 372–382, pp. 662–714.
10. Peretti, A.; Günther, D.; Graber, A.L. The Beryllium Treatment of Fancy Sapphires with a New Heat-treatment Technique (Part B). *Contrib. Gemol.* **2003**, *8*, 21–34.
11. Taran, M.N.; Koch-Müller, M.; Langer, K. Electronic absorption spectroscopy of natural (Fe²⁺, Fe³⁺)-bearing spinels of spinel s.s.-hercynite and gahnite-hercynite solid solutions at different temperatures and high-pressures. *Phys. Chem. Miner.* **2005**, *32*, 175–188. [[CrossRef](#)]
12. Fregola, R.A.; Skogby, H.; Bosi, F.; D’Ippolito, V.; Andreozzi, G.B.; Halenius, U. Optical absorption spectroscopy study of the causes for color variations in natural Fe-bearing gahnite: Insights from iron valency and site distribution data. *Am. Miner.* **2014**, *99*, 2187–2195. [[CrossRef](#)]
13. D’Ippolito, V.; Andreozzi, G.B.; Halenius, U.; Skogby, H.; Hametner, K.; Günther, D. Color mechanisms in spinel: Cobalt and iron interplay for the blue color. *Phys. Chem. Miner.* **2015**, *42*, 431–439. [[CrossRef](#)]
14. Gorghinian, A.; Mottana, A.; Rossi, A.; Oltean, F.M.; Esposito, A.; Marcelli, A. Investigating the colour of spinel: 1. Red gem-quality spinels (“balas”) from Ratnapura (Sri Lanka). *Rend. Lincei* **2013**, *24*, 127–140. [[CrossRef](#)]
15. Andreozzi, G.B.; D’Ippolito, V.; Skogby, H.; Halenius, U.; Bosi, F. Color mechanisms in spinel: A multi-analytical investigation of natural crystals with a wide range of coloration. *Phys. Chem. Miner.* **2019**, *46*, 343–360. [[CrossRef](#)]
16. Boris, C.; Benjamin, R.; Emmanuel, F.; Phillipe, R.; Jean-Luc, D. Blue spinel from the Luc Yen District of Vi-etnam. *Gems Gemol.* **2015**, *51*, 2–17.
17. Kane, R.E.; Kammerling, R.C. Status of Ruby and Sapphire Mining in the Mogok Stone Tract. *Gems Gemol.* **1992**, *28*, 152–174. [[CrossRef](#)]
18. Mitchell, A.H.G.; Htay, M.T.; Htun, K.M.; Win, M.N.; Oo, T.; Hlaing, T. Rock relationships in the Mogok metamorphic belt, Tatkon to Mandalay, central Myanmar. *J. Asian Earth Sci.* **2007**, *29*, 891–910. [[CrossRef](#)]
19. Keller, P.C. The Rubies of Burma: A Review of the Mogok Stone Tract. *Gems Gemol.* **1983**, *19*, 209–219. [[CrossRef](#)]
20. Giuliani, G.; Fallick, A.E.; Boyce, A.J.; Pardieu, V.; Pham, V.L. Pink and Red Spinel in Marble: Trace Elements, Oxygen Isotopes, and Sources. *Can. Miner.* **2017**, *55*, 743–761. [[CrossRef](#)]
21. Palke, A.C.; Sun, Z.Y. What Is Cobalt Spinel Unraveling the Causes of Color in Blue Spinel. *Gems Gemol.* **2018**, *54*, 262.
22. White, W.B.; DeAngelis, B.A. Interpretation of the vibrational spectra of spinels. *Spectrochim. Acta Part A* **1967**, *23*, 985–995. [[CrossRef](#)]
23. Farmer, V.C. *The Infrared Spectra of Minerals*; Mineralogical Society: Chantilly, VA, USA, 1974.
24. Vernidub, N.M.; Pasechnik, Y.A.; Shportko, K.V. Reststrahlen Spectroscopy of MgAl₂O₄ Spinel. *Semicond. Phys. Quantum Electron. Optoelectron.* **2002**, *5*, 95–100.
25. O’Horo, M.P.; Frisillo, A.L.; White, W.B. Lattice vibrations of MgAl₂O₄ spinel. *J. Phys. Chem. Solids* **1973**, *34*, 23–28. [[CrossRef](#)]
26. Shebanova, O.N.; Lazor, P. Raman study of magnetite (Fe₃O₄): Laser-induced thermal effects and oxidation. *J. Raman Spectrosc.* **2003**, *34*, 845–852. [[CrossRef](#)]

27. D'Ippolito, V.; Andreozzi, G.B.; Bersani, D. Raman fingerprint of chromate, aluminate and ferrite spinels. *J. Raman Spectrosc.* **2015**, *46*, 1255–1264. [[CrossRef](#)]
28. Lenaz, D.; Lughì, V. Raman study of $\text{MgCr}_2\text{O}_4\text{-Fe}^{2+}\text{Cr}_2\text{O}_4$ and $\text{MgCr}_2\text{O}_4\text{-MgFe}_2^{3+}\text{O}_4$ synthetic series: The effects of Fe^{2+} and Fe^{3+} on Raman shifts. *Phys. Chem. Miner.* **2013**, *40*, 491–498. [[CrossRef](#)]
29. Schmetzer, K.; Haxel, C.; Bank, H. Colour of natural spinels, gahnospinel and gahnites. *Neues Jahrb. Fur Mineral.* **1989**, *160*, 159–180.
30. Lenaz, D.; Skogby, H.; Princivalle, F.; Halenius, U. Structural changes and valence states in the $\text{MgCr}_2\text{O}_4\text{-FeCr}_2\text{O}_4$ solid solution series. *Phys. Chem. Miner.* **2004**, *31*, 633–642. [[CrossRef](#)]
31. Halenius, U.; Andreozzi, G.B.; Skogby, H. Structural relaxation around Cr^{3+} and the red-green color change in the spinel (sensu stricto)-magnesiochromite ($\text{MgAl}_2\text{O}_4\text{-MgCr}_2\text{O}_4$) and gahnitezincochromite ($\text{ZnAl}_2\text{O}_4\text{-ZnCr}_2\text{O}_4$) solid-solution series. *Am. Miner.* **2010**, *95*, 456–462. [[CrossRef](#)]
32. Malsy, A.K.; Karampelas, S.; Schwarz, D.; Klemm, L.; Armbruster, T. Tuan DA Orange-red to orange-pink gem spinels from a new deposit at Lang Chap (Tan Huong-Truc Lau), Vietnam. *J. Gemmol.* **2012**, *33*, 19–27. [[CrossRef](#)]

Disclaimer/Publisher's Note: The statements, opinions and data contained in all publications are solely those of the individual author(s) and contributor(s) and not of MDPI and/or the editor(s). MDPI and/or the editor(s) disclaim responsibility for any injury to people or property resulting from any ideas, methods, instructions or products referred to in the content.